Finite-Element Model for the Thermoelastic Analysis of Large Composite Space Structures

J.D. Lutz,* D.H. Allen,† and W.E. Haisler‡
Texas A&M University, College Station, Texas

A finite-element model that performs an integrated thermoelastic analysis of large composite space structures is outlined. The model allows for temperature gradients within structural member cross sections and for bending of the members themselves. Nonlinear effects such as radiation boundary conditions and temperature-dependent material properties are also included. Once the model is outlined, a preliminary investigation into the importance of thermally induced forces and moments is carried out. The problem chosen is that of a long cantilevered lattice boom in a geosychronous orbit. For the structure and loading chosen, no significant dynamic responses, such as vibration, occurred. In addition, thermally induced axial forces were the predominant type of loading. For this problem, thermally induced moments could be neglected. The magnitude of axial stresses generated by the transition from shadow to sunlight is on the order of 30% of yield stress.

Nomenclature

A	= cross-sectional area of a structural member
B	= boundary of cross-sectional area
c_p	= specific heat
E	= Young's modulus
G	= modulus of rigidity
I_m	= mass inertia
I_{yy}, I_{zz}	= moments of inertia about y and z axes
J	= polar moment of inertia
k	= thermal conductivity
L	= length of a structural member
M_y	= mechanical moment about y axis
M_z	= mechanical moment about z axis
M_y^T	= thermally induced moment about y axis
M_z^T	= thermally induced moment about z axis
n_x, n_y, n_z	= direction normals
P	= mechanically induced axial load
P^T	= thermally induced axial force
q	= normal incident flux
T	= temperature
T_0	= temperature in an unstrained state
T_r	= radiation reference temperature
t	= time
u, v, w	= displacements in coordinate directions
x, y, z	= coordinate directions
α_T	= coefficient of thermal expansion
ϵ	= emissivity
Θ	= rotation about x axis
ρ	= density
σ	= Boltzman's constant
σ_{xx}	= axial stress

Received March 20, 1986; presented as Paper 86-0875 at the AIAA/ASME/ASCE/AHS 27th Structures, Structural Dynamics and Materials Conference, San Antonio, TX, May 19-21, 1986; revision received Oct. 16, 1986.

†Associate Professor, Aerospace Engineering Department. Member AIAA.

‡Professor, Aerospace Engineering Department. Associate Fellow AIAA.

Introduction

In the next few decades, large space structures will be placed into Earth orbit. Because these vehicles will not be subjected to the launch environment but will be either deployed or constructed from materials carried into orbit, design will be based on criteria previously considered secondary. These criteria combined with new performance requirements will result in large lattice-type structures that utilize high-strength, low-density materials such as graphite fiber/polymeric matrix composites.

Under anticipated thermal loading conditions, structural members made from advanced fiber/matrix materials respond quite differently compared to those made from the more traditional metallic materials. Past research indicates that a graphite/epoxy structural member modeled as a slender thin-walled tube experiences a significant temperature gradient around its perimeter.[1] In addition, such a member will have a negligible temperature gradient along its length.[2] Both of these responses are due to the low thermal conductivity found in fiber/matrix materials.

A large temperature gradient through the cross section of a member produces bending. This is important for two reasons: 1) bending reduces the maximum allowable load a member can sustain, 2) bending may lead to fatigue, which is important in predicting the long-term behavior of the material.[3]

In this paper, the development of a finite-element model capable of performing an integrated thermoelastic analysis is outlined. This model is specifically designed for lattice-type structures made from low-conductivity materials, wherein the temperature distribution within a structural member varies through its cross section but not along its length. In addition, initial studies are carried out to determine the significance of thermally induced bending and extension. For this purpose, a typical space structure is developed and its thermal/structural response examined for two different load cases. Further details are given in Ref. 4.

Background

A general thermoelastic analysis of a large space structure is complicated by several factors: 1) there is the coupling between the temperature and displacement fields; 2) the thermal analysis itself is highly nonlinear due to the inclusion of radiation boundary conditions and temperature-dependent material properties; 3) the thermal loading is constantly changing due to varying Earth/structure/sun orientation;

and 4) geometrical factors such as shadowing and interelement radiation can exist.

In the model developed here, several simplifying assumptions are made. To begin with, the temperatures are assumed to be independent of deformation, that is uncoupled. This allows the temperature field to be solved for first and then used as input to the structural analysis. All structures are assumed to be of open lattice-work construction with long thin members sparsely located. This allows for the omission of interelement radiation and shadowing. The structural members are modeled as thin-walled cylinders of constant cross-sectional and material properties. Furthermore, because temperatures within these members vary through their cross section and not along their length, each member may be treated as an isolated body, absorbing thermal radiation and, in turn, emitting its own radiation, as shown in Fig. 1.

The thermal loading is also simplified by requiring all structures to be in a high Earth orbit. At high altitudes, Earth-emitted and Earth-reflected radiation are negligible. Furthermore, if structures are assumed to have a space-fixed orientation, the solar flux is both constant in magnitude and direction during the sunlit portion of an orbit.

Model Development

The finite-element model consists of five sections. The algorithm, shown schematically in Fig. 2, is as follows. On a given time step, the proper thermal loads are first evaluated. In the second step, finite elements are used to construct the temperature fields through selected cross sections. The two-dimensional heat-transfer problem within a cross section is shown in Fig. 3 and governed by Eqs. (1) and (2).[5] These equations neglect internal heat generation, but include temperature-dependent material properties, namely k_y, k_z, and c_p. Solving the nonlinear heat-transfer problem in a single cross section per member is prohibitively expensive. However, it is expected that the repetitive nature of the proposed lattice structures will allow a greatly reduced thermal analysis, wherein the results from a few selected cross sections are used throughout the structure,

$$\rho c_p \frac{\partial T}{\partial t} = \frac{\partial}{\partial y}\left(k_y \frac{\partial T}{\partial y}\right) + \frac{\partial}{\partial z}\left(k_z \frac{\partial T}{\partial z}\right) \tag{1}$$

$$k_y \frac{\partial T}{\partial y} n_y + k_z \frac{\partial T}{\partial z} n_z = q\alpha + \epsilon\sigma\left(T_r^4 - T^4\right) \tag{2}$$

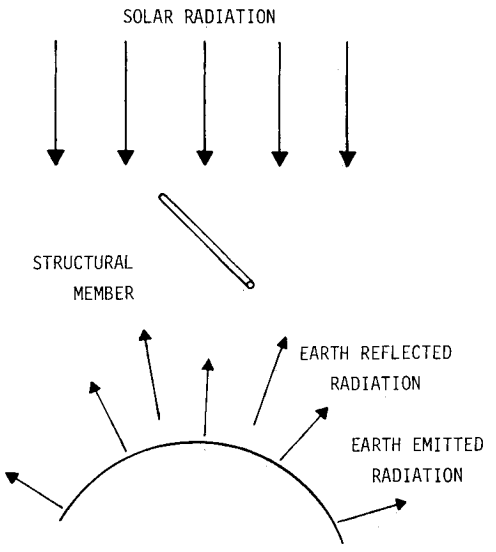

Fig. 1 A structural element in space environment.

Within a cross section, heat is transferred by conduction around the perimeter and radiation from the inner surfaces. In addition, heat is lost to space through radiation from the outer surfaces. The third step in the procedure involves utilizing the resulting temperature fields to calculate thermal forces and moments using the following relations[5,6]:

$$P^T = \int_A E\alpha_T (T - T_0)\,dA \tag{3}$$

$$M_y^T = \int_A E\alpha_T (T - T_0) z\,dA \tag{4}$$

$$M_z^T = \int_A E\alpha_T (T - T_0) y\,dA \tag{5}$$

These loads are initially determined in the local coordinates of their cross section. They are then transformed in the fourth step into the global coordinates of the structure to be used as input for the structural analysis.

Equations (3-5) arise from the utilization of the Euler-Bernoulli beam theory, in which cross sections are assumed to remain plane and normal to the centroidal axis during deformation.[5,6] Substituting Eqs. (3-5) into the uniaxial

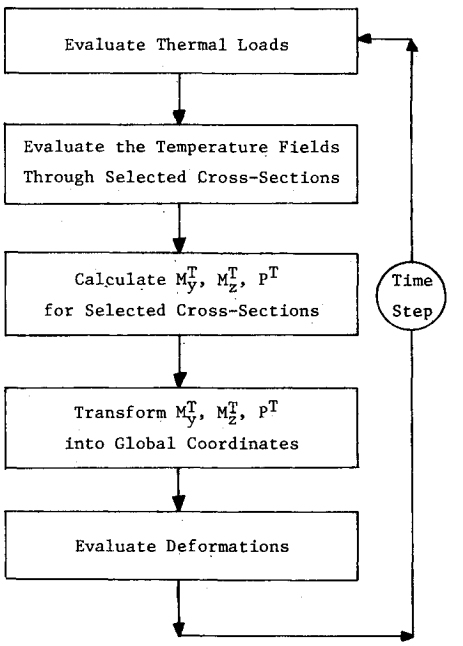

Fig. 2 Algorithm schematic.

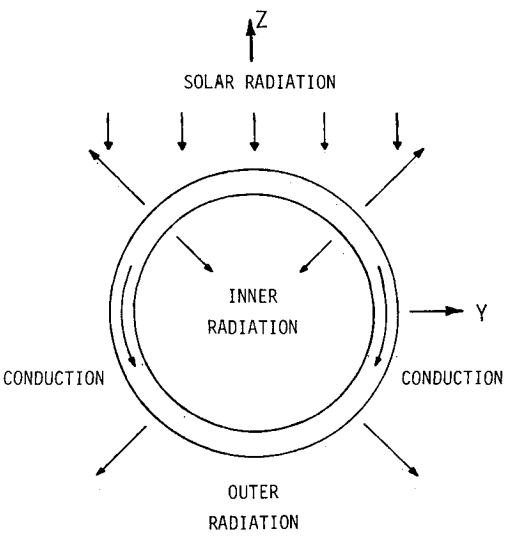

Fig. 3 Heat transfer in a selected cross section.

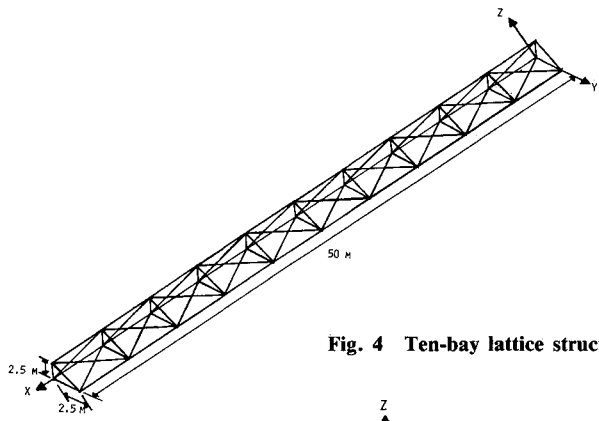

Fig. 4 Ten-bay lattice structure.

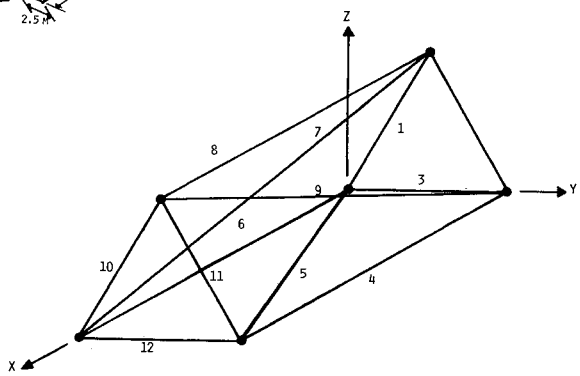

Fig. 5 Finite-element mesh for structural response of the first bay.

Table 1 Material properties for graphite AS/epoxy composite[9]

T,K	k,W/m·K	c_p, J/kg·K
0	0.0	0.419
120	3.834	338.0
170	5.993	479.0
220	8.032	620.0
270	9.714	783.0
330	10.14	976.0
400	11.14	1080.
810	16.98	1660.

$E=4.5\times10^{10}$N/m^2
$G=1.5\times10^{10}$N/m^2
$\rho=1.633\times10^{3}$kg/m^3
$\alpha=0.916$
$\epsilon=0.800$
$\alpha_T=7.290\times10^{-7}$m/m·K

Table 2 Orbital data

	GEO	LEO
Period, s	86,400	5400
Altitude, km	35,800	280
Umbra, s	4,200	2200
Penumbra, s	130	8

Table 3 Cross-section numbers for first-bay elements

Element No.	Cross-section No.	Element No.	Cross-section No.
1	2	7	3
2	2	8	1
3	1	9	3
4	1	10	2
5	1	11	2
6	1	12	1

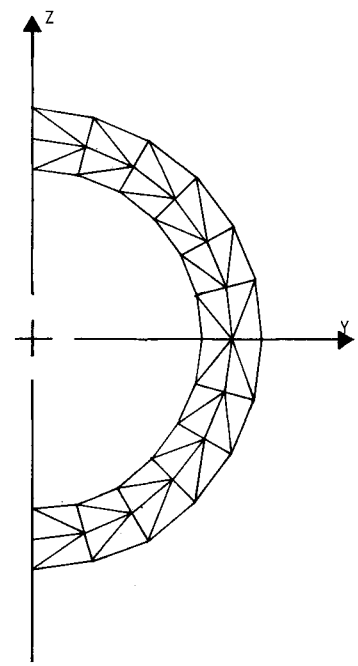

Fig. 6 Finite-element mesh for heat transfer in a selected cross section.

stress-strain relations and integrating over the beam cross section results in[6]

$$\sigma_{xx}=\frac{(P+P^T)}{A}-\frac{(M_z-M_z^T)}{I_{zz}}y+\frac{(M_y-M_y^T)}{I_{yy}}z-E\alpha_T(T-T_0) \tag{6}$$

In statically indeterminate structures, the mechanical resultants P, M_y, and M_z are induced by temperature gradients (in addition to P^T, M_y^T, and M_z^T) in order to maintain equilibrium in the structure. In fact, it is not uncommon for the mechanical resultants to be large compared to the thermal resultants, even in the case where heating is the only external loading on the structure.

The structural (or deformation) analysis is the final step in the algorithm shown in Fig. 3. It is developed from application of standard finite-element formulations to the governing equations of beam motion,[7,8]

$$\frac{\partial}{\partial t}\left(\rho A\frac{\partial u}{\partial t}\right)-\frac{\partial}{\partial x}\left(EA\frac{\partial u}{\partial x}\right)-\frac{\partial P^T}{\partial x}=0 \tag{7}$$

$$\frac{\partial}{\partial t}\left(I_m\frac{\partial\Theta}{\partial t}\right)-\frac{\partial}{\partial x}\left(JG\frac{\partial\Theta}{\partial x}\right)=0 \tag{8}$$

$$\frac{\partial}{\partial t}\left(\rho A\frac{\partial v}{\partial t}\right)-\frac{\partial^2}{\partial x^2}\left(EI_{zz}\frac{\partial^2 v}{\partial x^2}\right)-\frac{\partial^2 M_z^T}{\partial x^2}=0 \tag{9}$$

$$\frac{\partial}{\partial t}\left(\rho A\frac{\partial w}{\partial t}\right)-\frac{\partial^2}{\partial x^2}\left(EI_{yy}\frac{\partial^2 w}{\partial x^2}\right)-\frac{\partial^2 M_y^T}{\partial x^2}=0 \tag{10}$$

Problem Summary

In order to demonstrate the use of the model, and as an initial investigation into the significance of thermal loads, consider the following problem. A long cantilevered boom structure is in a geosychronous orbit about the Earth. During an orbit, the boom moves from the Earth's shadow into sunlight and back into shadow. While transitioning from one

thermal environment to another, the boom undergoes deformation and possibly vibration.

The structure, shown in Fig. 4, is 50 m long and composed of 10 identical bays of triangular cross section. Each bay is 5 m long and 2.5 m on a side. The structural members themselves are thin-walled cylinders and, except for length, identical to one another. The cross section diameter is 0.1 m and the thickness is 0.004 m. All members are assumed to be made from graphite AS/epoxy with the properties given in Table 1. Although it is quite possible that some orthotropy will be built into these structural members due to their predominantly uniaxial stress state, in order to simplify the analysis in the current application, it has been assumed that the members are quasi-isotropic. Long tube quasi-isotropic members can be fabricated in filament winding processes.

Two load cases are examined: the first examines a boom structure originating in sunlight and moving into shadow and the second the same boom moving from shadow into sunlight.

Case 1

For the first case, the structure is assumed to be in thermal equilibrium and stress free in the sunlit portion of its orbit. This corresponds to an assembly in sunlight. Because of the different orientations of the various members, thermal equilibrium corresponds to a state in which the temperatures in the various members are not the same. At time $t=0$, the structure moves into shadow and deforms until reaching a new thermal equilibrium. Because the structure is in a geosychronous orbit, the time to cross the penumbra is negligible and the transition into shadow is assumed to be instantaneous, as shown in Table 2. Furthermore, all initial cross-sectional temperature gradients are neglected and the initial temperature of each member is its radiation equilibrium temperature, found by equating the flux and radiation boundary terms in Eq. (2). Due to the different initial temperatures in the members, the members radiate heat at differing rates.

Case 2

In this case, a transition from shadow into sunlight is considered. Here, the boom is undeformed and at an initial uniform temperature in all members of 77 K. At time $t=0$, the boom moves into sunlight and deforms. In a geosychronous orbit, penumbra effects are ignored and the solar flux is applied instantaneously and uniformly along the length of the boom. The solar flux is considered to act in the negative z direction with respect to the global coordinates shown in Fig. 4. Its magnitude is given as 1.4 kW/m^2.

Finite-Element Model

Structural modeling of the boom is straightforward. The finite-element representation of the boom uses one space frame element per member. This results in a mesh of 33 nodes and 93 elements. The mesh for the first bay is shown in Fig. 5.

By comparison, thermal modeling of the structure appears quite complex. However, it can be greatly simplified. Because each bay is identical to the next and the incident flux is both uniform along the length of the boom and constant with time, only one bay need be modeled. The temperature distribution in that bay is then applicable throughout the boom. In addition, the thermal analysis of the bay may be simplified. Upon examination of the first bay, shown in Fig. 5, it is apparent that all 12 members can be assigned to one of three groups based on their orientation with respect to the direction of the solar flux. This grouping is shown in Table 3. It should be noted that, if cross-sectional or material properties varied from member to member, additional subgroupings would be necessary. For this simplified case, modeling only one cross section from each group is needed for determining the temperature distribution in a bay. Therefore, the thermal analysis of the entire boom has been reduced to examining three member cross sections.

The finite-element representation for heat conduction in a cross section is shown in Fig. 6. Here, only half the cross section need be modeled if the local axes of the cross section are aligned with the solar flux vector. The mesh used consists of 48 constant thermal gradient elements and 39 nodes.

Discussion of Results

For both load cases, examples of thermally induced loads vs time are presented. These curves represent the induced mechanical loads applied throughout the structure. Also, the resulting axial stress history in a selected member is given as a ratio of maximum axial stress over tensile strength. This

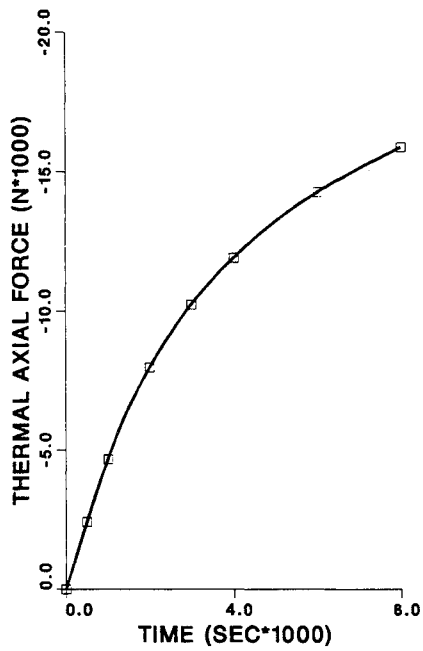

Fig. 7 Induced axial force in cross section for case 1.

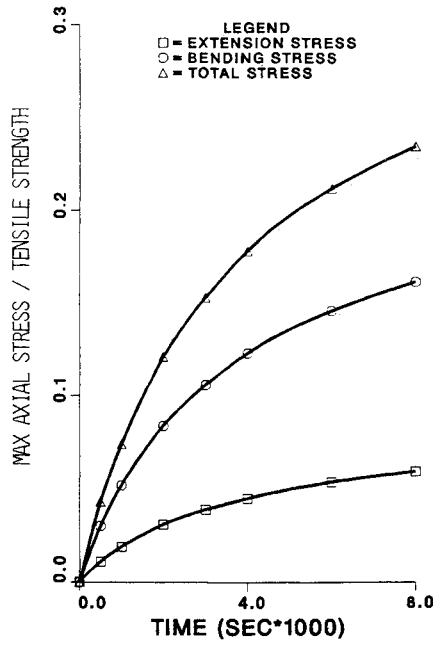

Fig. 8 Ratio of maximum axial stress to tensile strength in element 4 for case 1.

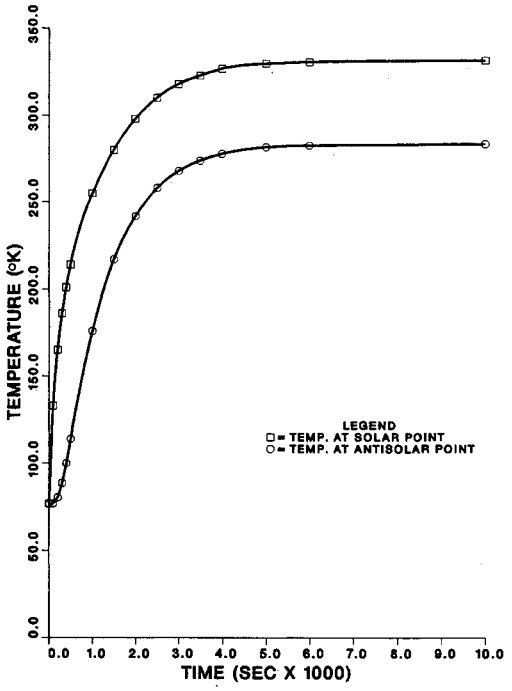

Fig. 9 Temperature versus time at solar and antisolar points for cross section 1.

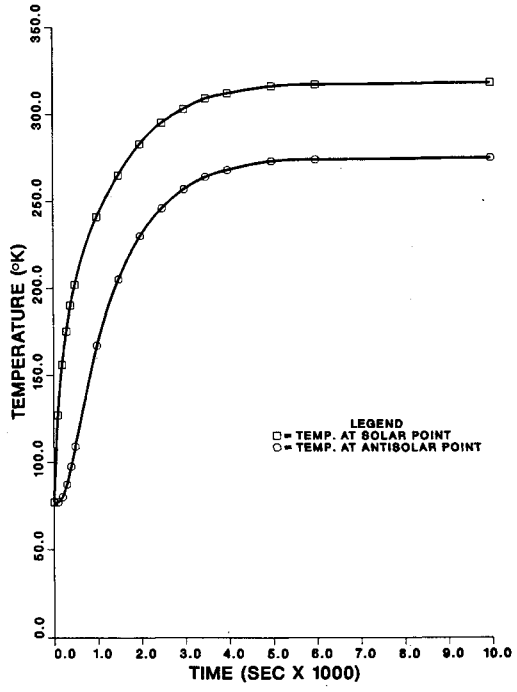

Fig. 10 Temperature versus time at solar and antisolar points for cross section 2.

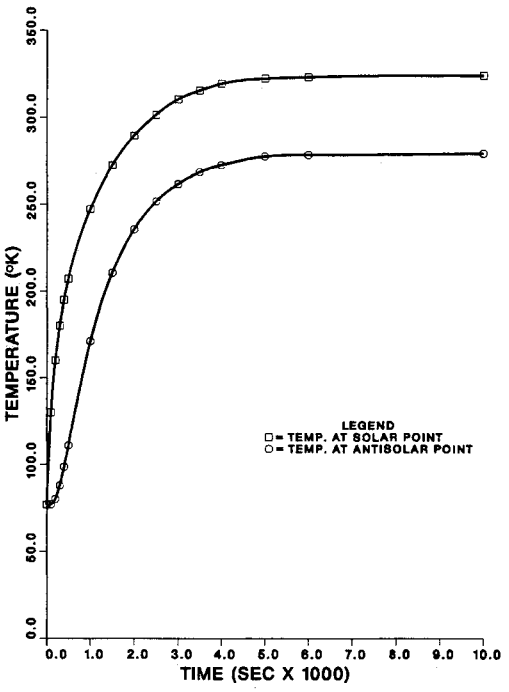

Fig. 11 Temperature versus time at solar and antisolar points for cross section 3.

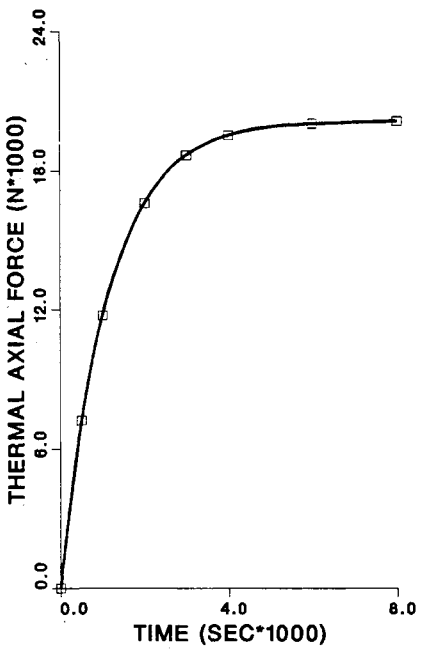

Fig. 12 Induced axial force in cross section 1 for case 2.

stress is further divided into bending stress and stress due to extension. Examples of temperature variation are given for three members in case 2. For graphite AS/epoxy, tensile strength is approximately 1 GPa (150 ksi).

Case 1

In Fig. 7, the thermal axial force vs time induced in all members using cross section 1 (see Table 3) is given. As expected, the magnitude of the compressive force increases smoothly as the cross section cools. Because the initial temperature is assumed to be uniform in each member, the induced thermal moment in this cross section is very small. However, the variation in temperatures between the members induces mechanical forces and moments that are significant.

The resulting axial stress for this case is given in Fig. 8 for structural element 4. The axial stress, as calculated in Eq. (6), accounts for both mechanical and thermal forces and moments. This element is located at the cantilevered end of the boom and carries a higher level of stress than those located near the free end. It is evident that stress levels are not overly large for the structure chosen. At a time corresponding to that required to cross the umbra, the maximum axial stress in element 4 is 20% of tensile strength. In addition, the stress increases monotonically with the applied load, indicating no oscillatory motion. Forces and moments

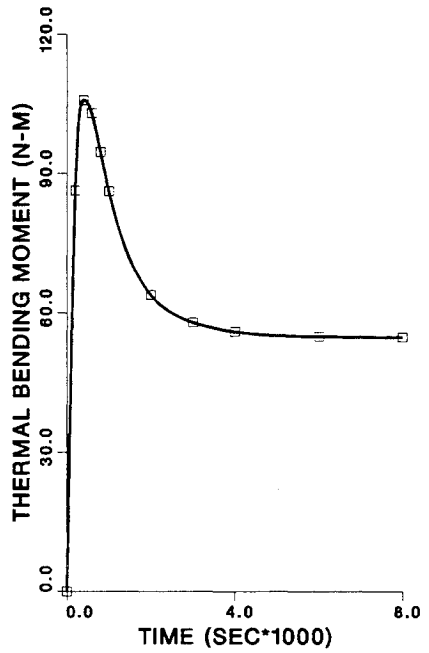

Fig. 13 Induced bending moment in cross section 1 for case 2.

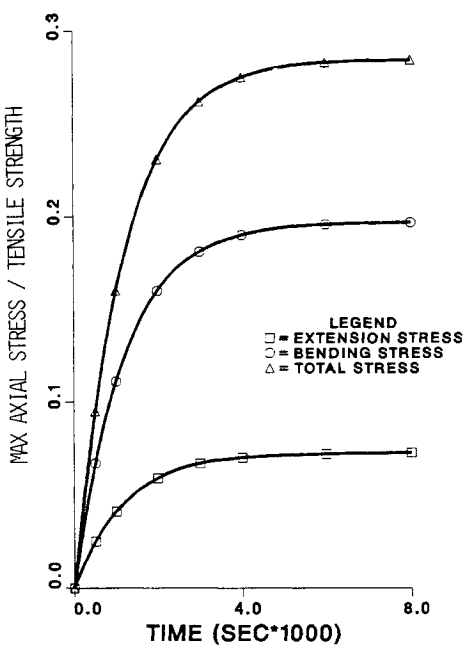

Fig. 14 Ratio of maximum axial stress to tensile strength in cross section 1 for case 2.

induced in the other two cross sections behave similarly to element 4, but with smaller magnitudes.

Case 2

For Case 2, significant thermal gradients occur in all three cross sections, as shown in Figs. 9–11. For this case, significant thermal forces and bending moments are produced by the thermal loading. For cross section 1, the induced thermal loads are given in Figs. 12 and 13. The axial force increases smoothly and approaches a steady-state value at around 8000 s. This is then the time required for the cross section to regain thermal equilibrium. The induced thermal moment behaves quite differently. An early peak is reached within the first 500 s due to the lag in the heat transfer around and through the cross section. At this point, the temperature gradient has peaked. After a maximum is reached, the moment decreases to steady state at 8000 s.

Figure 14 gives the maximum axial stress obtained from Eq. (6) induced in structural element 4 by the aforementioned loads. Steady-state stress values are on the order of 30% of tensile strength. Also, the stress increases smoothly, indicating no oscillation. It is interesting to note that the stress, and therefore deformations, are in phase with the thermal axial forces. This indicates that thermal bending moments do not produce significant axial stresses. However, the thermal axial loads induce significant mechanical bending moments in the structure. Therefore, it is concluded that structural bending cannot be neglected. The results from the other two selected cross sections are similar, but with smaller magnitudes for this case.

Conclusions

This study has attempted to investigate the significance of thermal loading on large composite space structures by examining thermoelastic responses. For this purpose, an integrated finite-element model for performing an uncoupled thermoelastic analysis has been outlined. This model accounts for cross-sectional temperature gradients within members and for nonlinear effects such as radiation boundary conditions and temperature-dependent material properties. Initial studies using this model have been carried out to determine the significance of thermally induced loads. Although only limited studies have been conducted, several conclusions concerning thermal loads have been reached.

First, the present research indicates that, for the structure modeled here, there is no significant dynamic response due to the thermal loading associated with entering and exiting the Earth's shadow. Although the thermal environment changes instantaneously, thermally induced axial forces and bending moments are produced in a much slower monotonic fashion. These loads require several thousand seconds to reach their steady-state values. It has been estimated that even very large flexible structures will have their first fundamental frequencies in the range of 0.01–10.0 Hz.[10] The fundamental periods corresponding to these frequencies prove much too small to allow excitation from the induced thermal loads.

Furthermore, in both cases studied, although the thermal moments are very small, the thermal axial forces induce significant mechanical bending in the structure. However, the thermally induced loads are very dependent on the initial reference state chosen. Choosing a reference temperature near the steady-state temperature reduces the induced axial forces while leaving the bending moments unchanged. Therefore, it is not yet clear if thermally induced moments, and likewise cross-sectional temperature gradients, can be neglected.

Finally, the magnitude of the thermally induced axial stresses is less than 30% of tensile strength. Although this cannot be neglected, it is not excessive. Also, these stress levels could become very important in conjunction with stresses produced by maneuvering and docking.

Although the study presented here is only a preliminary one, several important trends are evident. However, the evaluation of thermally induced axial and bending forces depends on many factors and will require more investigation in order to determine their real significance in thermoelastic responses.

Acknowledgment

The authors wish to express their thanks to the U.S. Air Force Office of Scientific Research, which sponsored this research under Contract F49620-83-C-0067.

References

[1]Brogren, E.W., Barclay, D.L., and Straayer, J.W., "Simplified Thermal Estimation Techniques for Large Space Structures," NASA-CR-145253, 1977.

[2]Thornton, E.A., Mahaney, J., and Dechaumphai, P., "Finite Element Thermal-Structural Modeling of Orbiting Truss Structures," *Large Space Systems Technology,* Third Annual Technical Review, Langley Research Center, Hampton, VA, 1981.

[3]Thornton, E.A., "Thermal-Structural Analysis of Large Space Structures: A Review of Recent Advances," AFWAL-TR-82-3048, 1982.

[4]Lutz, J.D., "A Finite Element Model for Transient Thermal/Structural Analysis of Large Composite Space Structures," M.S. Thesis, Texas A&M University, College Station, 1986.

[5]Boley, B.A., and Weiner, J.H., *Theory of Thermal Stresses,* Wiley, New York, 1960.

[6]Allen, D.H., and Haisler, W.E., *Introduction to Aerospace Structural Analysis,* Wiley, New York, 1984.

[7]Reddy, J.N., *An Introduction to the Finite Element Method,* McGraw-Hill, New York, 1984.

[8]Bathe, K.J., *Finite Element Procedures in Engineering Analysis,* Prentice-Hall, Englewood Cliffs, NJ, 1982.

[9]"Magnamite Graphite Fibers Proven High Performance," Hercules, Inc., Magna, UT, 1981.

[10]Kalyanasundarum, S., Lutz, J.D., Haisler, W.E., and Allen, D.H., "Effect of Degradation of Material Properties on the Dynamic Response of Large Space Structures," *Journal of Spacecraft and Rockets,* Vol. 23, May 1986, pp. 297-302.